

# PURIFIED SASE UNDULATOR CONFIGURATION TO ENHANCE THE PERFORMANCE OF THE SOFT X-RAY BEAMLINE AT THE EUROPEAN XFEL

Svitozar Serkez, Vitali Kocharyan, Evgeni Saldin, Igor Zagorodnov  
 Deutsches Elektronen-Synchrotron (DESY), Hamburg, Germany  
 Ilya Agapov, Gianluca Geloni  
 European XFEL GmbH, Hamburg, Germany

## Abstract

The purified SASE (pSASE) undulator configuration recently proposed at SLAC promises an increase in the output spectral density of XFELs. In this article we study a straightforward implementation of this configuration for the soft x-ray beamline at the European XFEL. A few undulator cells, resonant at a subharmonic of the FEL radiation, are used in the middle of the exponential regime to amplify the radiation, while simultaneously reducing the FEL bandwidth. Based on start- to-end simulations, we show that with the proposed configuration the spectral density in the photon energy range between 1.3 keV and 3 keV can be enhanced of an order of magnitude compared to the baseline mode of operation. This option can be implemented into the tunable-gap SASE3 baseline undulator without additional hardware, and it is complementary to the self-seeding option with grating monochromator proposed for the same undulator line, which can cover the photon energy range between about 0.26 keV and 1 keV.

## INTRODUCTION

The SASE3 beamline at the European XFEL will be operated in the photon energy range between 0.26 keV and at least 3 keV. A high level of longitudinal coherence is the key to upgrade the baseline performance. Self-seeding is a promising approach to significantly narrow the SASE bandwidth and to produce nearly transform-limited pulses [1]-[20]. The implementation of this method in the soft x-ray wavelength range necessarily involves gratings as dispersive elements, which may be installed in the SASE3 undulator without perturbing the electron focusing system and could cover the spectral range between about 0.26 keV and 1 keV [18]- [19]. In order to provide a high level of longitudinal coherence in the photon energy range between 1 keV and 3 keV, proposals exist to narrow the SASE bandwidth at the European XFEL by combining self-seeding and fresh bunch techniques. However, this requires installing additional hardware in the undulator system [21, 22]. Here we explore a simpler method to reach practically the same result without further changes in the undulator system. The solution is based in essence on the purified SASE (pSASE) technique proposed at SLAC [23], and naturally exploits the gap tunability of the SASE3 undulator. In the pSASE configuration, a few undulator cells resonant at a subharmonic of the FEL radiation, called altogether the "slippage-boosted

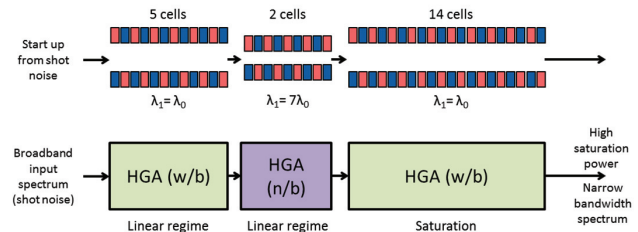


Figure 1: The pSASE undulator configuration proposed for the SASE3 beamline, which is expected to operate in the photon energy range between 1.3 keV and 3 keV.

section", are used in the high-gain linear regime to reduce the SASE bandwidth. The final characteristics of a pSASE source are a compromise between high output power, which can be reached with a conventional SASE undulator source resonant at the target wavelength, and narrow bandwidth, which can be reached with harmonic lasing [24]- [28]. We demonstrate that it is possible to cover the energy range between 1.3 keV and 3 keV using the nominal European XFEL electron beam parameters, and to reduce the SASE bandwidth by a factor 5, still having the same output power as in the baseline SASE regime. Note that the slippage-boosted section is tuned to a subharmonic (the fifth, or the seventh) of the FEL radiation. Therefore, the choice of the lowest pSASE photon energy considered in this article, 1.3 keV, is dictated by the minimal photon energy (0.26 keV) that can be reached in the conventional SASE regime.

A more detailed treatment can be found in [29].

## FEL STUDIES

A schematic layout of the proposed pSASE configuration for the SASE3 undulator at the European XFEL is illustrated in Fig. 1 and consists of three parts which will be called U1 (5 cells), U2 (2 cells) and U3 (14 cells). We performed a feasibility study of the pSASE setup with the help of the FEL code Genesis 1.3 [30] running on a parallel machine. Results are presented for the SASE3 FEL line of the European XFEL, based on a statistical analysis consisting of 100 runs. The overall beam parameters used in the simulations are presented in Table 1.

The nominal beam parameters at the entrance of the SASE3 undulator, and the resistive wake inside the undulator are shown in Fig. 2, see also [31]. The evolution of the transverse electron bunch dimensions is plotted in Fig. 3.

Table 1: European XFEL Parameters Used in this Paper

	Units	
Undulator period	mm	68
Periods per cell	-	73
Total number of cells	-	21
Intersection length	m	1.1
Energy	GeV	10.5
Charge	nC	0.1

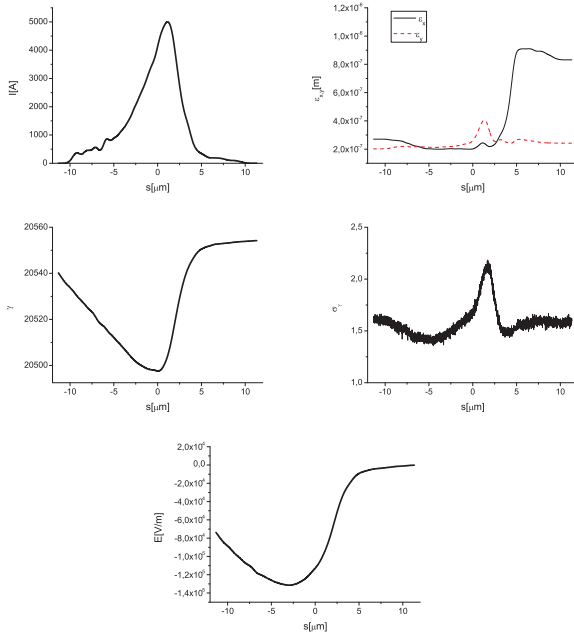


Figure 2: Results from electron beam start-to-end simulations at the entrance of SASE3. (First Row, Left) Current profile. (First Row, Right) Normalized emittance vs. position inside the electron beam. (Second Row, Left) Energy profile along the beam. (Second Row, Right) Electron beam energy spread profile. (Bottom row) Resistive wakefields in the SASE3 undulator.

The number of cells in the undulator U1 should be equal to five in order to optimize the final characteristics of the radiation pulse. The output power and spectrum after the first undulator tuned to 0.6 nm (the corresponding rms K value is 2.54) is shown in Fig. 4 for 100 runs. The average behavior

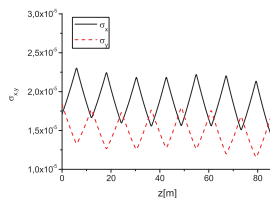


Figure 3: Evolution of the horizontal and vertical dimensions of the electron bunch (at maximum current value) vs. distance inside the SASE3 undulator.

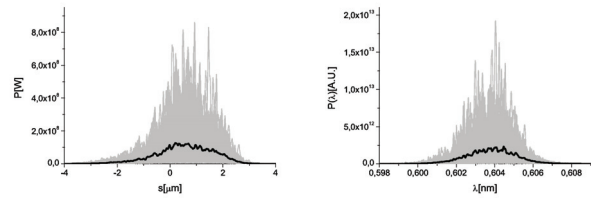


Figure 4: Power distribution and spectrum of the SASE soft x-ray radiation pulse at the exit of the first undulator part U1. Grey lines: single shot realization, black line: average over 100 realizations.

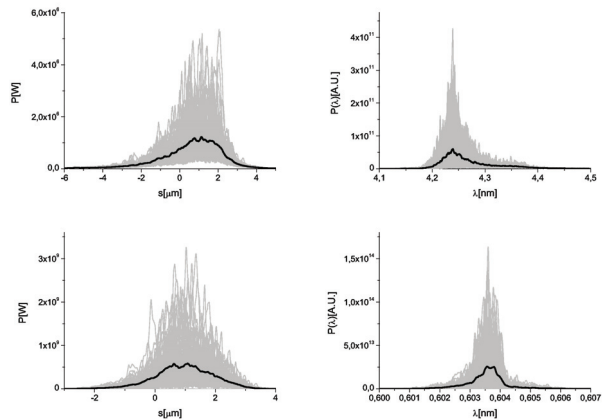


Figure 5: SASE radiation power and spectrum at the exit of the second undulator part U2 (slippage-booster section). The SASE radiation generated in U1 is purified in U2, which consists of 2 cells resonant at 4.2 nm. The fundamental radiation at 4.2 nm is seeded by shot noise. The harmonic radiation is seeded by that produced in U1. Top row: Results of numerical simulations for radiation at the fundamental produced in U2. Bottom row: Results of numerical simulations for harmonic radiation amplified in U2. Grey lines refer to single shot realizations, the black line refers to the average over a hundred realizations.

is rendered in black. The radiation field is first dumped at the exit of U1, and then further imported in the Genesis code for simulating the 7th harmonic interaction in U2, which is resonant at a fundamental of 4.2 nm. Together with the radiation pulse, also electron beam file generated using the values of energy loss and energy spread at the exit of U1 is fed in the simulation of the second undulator part. The Genesis 7th harmonic field and particle file are downloaded at the exit of the U2 undulator and used as input file for the Genesis simulations of the U3 undulator. As explained in the previous section, the length of the booster U2 is chosen to make sure that the FEL power at the fundamental wavelength is much lower than that at the chosen harmonic. The output power and spectrum of fundamental and harmonic radiation pulse after the U2 undulator tuned to 4.2 nm (the corresponding rms K value is 7.16, and can be achieved by reducing the undulator gap), that is the seventh subharmonic of the target wavelength, are shown in the left and right plot

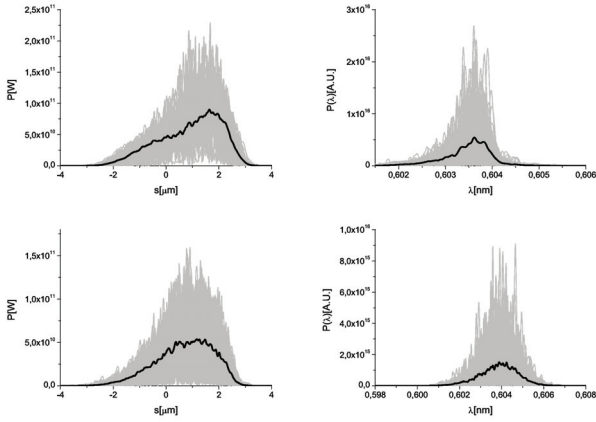


Figure 6: Power and spectrum produced in the pSASE mode (top row) and in the standard SASE mode (bottom row) at saturation without undulator tapering. Grey lines: single shot realization, black line: average over 100 realizations.

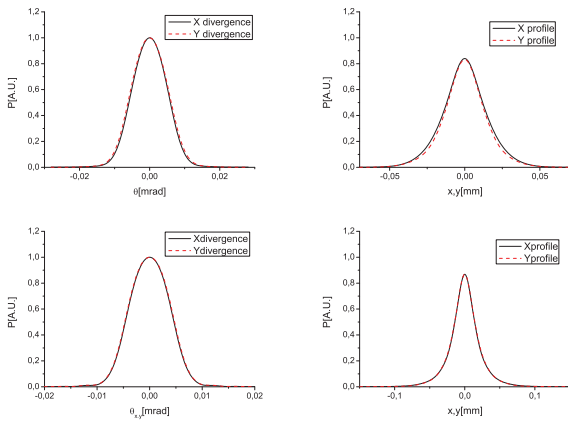


Figure 7: Distribution of the radiation pulse energy per unit surface and angular distribution of the pSASE radiation pulse energy at saturation (top row) and at the exit of the setup, including tapering (bottom row).

of Fig. 5. Since the FEL power at the fundamental wavelength of 4.2 nm, which is about 1 MW, is much lower than that at 0.6 nm, which is about 1 GW, phase shifters are not needed to suppress the lasing at fundamental harmonic.

The output undulator U3 consists of two sections. The first section is composed by a uniform undulator, the second section by a tapered undulator. The purified pulse is exponentially amplified passing through the first uniform

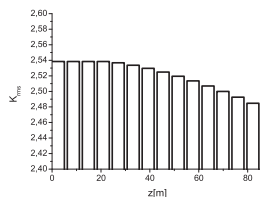


Figure 8: Tapering law.

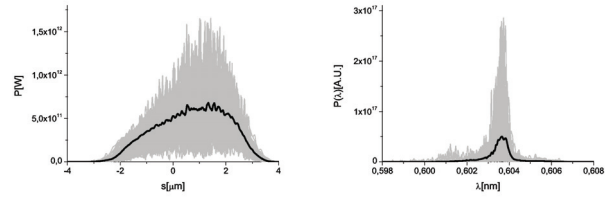


Figure 9: Power distribution and spectrum of the purified SASE soft x-ray radiation pulse at the exit of the setup, with tapering. Grey lines refer to single shot realizations, the black line refers to the average over a hundred realizations.

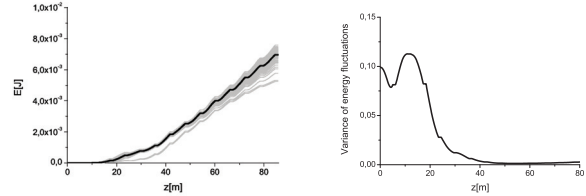


Figure 10: Evolution of the output energy in the photon pulse and of the variance of the energy fluctuation as a function of the distance inside the output undulator, with tapering. Grey lines refer to single shot realizations, the black line refers to the average over a hundred realizations.

part of the output undulator. This section is long enough, 5 cells, in order to reach saturation, which yields about 50 GW power Fig. 6 (top row). The radiation power profile and spectra for SASE3 undulator beamline working in the nominal SASE mode is shown in Fig. 6 (bottom row). As seen before, the power level for both modes of operation are similar, but the spectral density for the pSASE case is significantly higher than for the nominal SASE case. The size and divergence of the pSASE radiation pulse at saturation are shown in Fig. 7 (top row). In the second part of the output undulator U3, the purified FEL output is enhanced up to about 0.6 TW taking advantage of a taper of the undulator magnetic field over the last 9 cells after saturation. The tapering law is shown in Fig. 8. The output power and spectrum of the entire setup, at the exit of U3, is shown in Fig. 9. The size and divergence of the pSASE radiation pulse at the exit of the setup including undulator tapering are shown in the bottom row of Fig. 7. By inspection, one can see that the difference with the pSASE setup at saturation, shown in the top row of the same figure, is minimal. The evolution of the output energy in the photon pulse as a function of the distance inside the output undulator is reported in Fig. 10. The photon spectral density for the output TW-level pulse is about 30 times higher than that for the nominal SASE pulse at saturation.

## CONCLUSIONS

We studied the simple scheme proposed in [23] to significantly enhance the spectral brightness of a SASE FEL with the help of numerical simulations. Using the param-

eters for the soft x-ray beamline SASE3 at the European XFEL and a nominal electron bunch parameter set, we show that the SASE bandwidth at saturation can be reduced by a factor of five with respect to the proposed configuration of the baseline, variable gap SASE3 undulator. In addition to the example studied in [23], the purified radiation after saturation is further significantly amplified (we report an order of magnitude increase in power) in the last tapered part of SASE3 undulator. With this configuration, a pSASE FEL reaches TW peak power level with significantly enhanced brightness (about one order of magnitude) compared with the nominal SASE regime [32].

## REFERENCES

- [1] J. Feldhaus et al., "Possible application of X-ray optical elements for reducing the spectral bandwidth of an X-ray SASE FEL" *Optics. Comm.*, vol. 140, pp. 341-352, 1997.
- [2] E. Saldin et al., "X-ray FEL with a meV bandwidth", *NIM, ser. A*, vol. 475, pp. 357-362, Dec. 2001.
- [3] E. Saldin et al., "Optimization of a seeding option for the VUV free electron laser at DESY", *NIM, ser. A*, vol. 445, pp. 178-182, May 2000.
- [4] R. Treusch et al., "The seeding project for the FEL in TTF phase II", *DESY Ann. report*, 2001.
- [5] A. Marinelli et al., "Comparative study of nonideal beam effects in high gain harmonic generation and self-seeded free electron lasers", *Phys. Rev. ST Accel. Beams*, vol. 13, p. 070701, Jul 2010.
- [6] G. Geloni et al., "Scheme for generation of highly monochromatic X-rays from a baseline XFEL undulator", *DESY 10-033*, 2010.
- [7] Y. Ding et al., "Two-bunch self-seeding for narrow-bandwidth hard x-ray free-electron lasers" *Phys. Rev. ST Accel. Beams*, vol. 13, p. 060703, 2010.
- [8] G. Geloni et al., "A simple method for controlling the line width of SASE x-ray FELs", *DESY 10-053*, 2010.
- [9] G. Geloni et al., "A Cascade self-seeding scheme with wake monochromator for narrow-bandwidth x-ray FELs", *DESY 10-080*, 2010.
- [10] G. Geloni et al., "Cost-effective way to enhance the capabilities of the LCLS baseline", *DESY 10-133*, 2010.
- [11] J. Wu et al., "Staged self-seeding scheme for narrow bandwidth, ultra-short X-ray harmonic generation free electron laser at LCLS", *Proc. 34th Int. Free-Electron Laser Conf., Malmo, 2010, TUPB08*.
- [12] G. Geloni et al., "Generation of doublet spectral lines at self-seeded X-ray FELs", *DESY 10-199*, 2010, and *Optics Commun.*, vol. 284, p. 3348, 2011.
- [13] G. Geloni et al., "Production of transform-limited X-ray pulses through self-seeding at the European X-ray FEL", *DESY 11-165*, 2011.
- [14] G. Geloni et al., "A novel self-seeding scheme for hard X-ray FELs", *J. of Modern Optics*, vol. 58, p. 1391, 2011.
- [15] J. Wu et al., "Simulation of the Hard X-ray Self-seeding FEL at LCLS", *Proc. 33rd Int. Free-Electron Laser Conf., Shanghai, 2011, MOPB09*.
- [16] J. Amann et al., "Demonstration of self-seeding in a hard-X-ray free-electron laser", *Nature Photonics*, vol. 6, pp. 693-698, DOI:10.1038/NPHOTON.2012.180, 2012.
- [17] Yu. Shvyd'ko, R. Lindberg, "Spatiotemporal response of crystals in x-ray Bragg diffraction", *Phys. Rev. ST Accel. Beams*, vol. 15, p. 100702, Oct. 2012.
- [18] Y. Feng et al., "System design for self-seeding the LCLS at soft X-ray energies", *Proc. 34th Int. Free-Electron Laser Conf., Nara, Japan, 2012, TUOB10*.
- [19] S. Serkez et al., "Grating monochromator for soft X-ray self-seeding the European XFEL", *DESY 13-040*, Available: <http://arxiv.org/abs/1303.1392>, 2013.
- [20] G. Geloni et al., "Wake monochromator in asymmetric and symmetric Bragg and Laue geometry for self-seeding the European XFEL", *DESY 13-013*, 2013.
- [21] G. Geloni et al., "Conceptual design of an undulator system for a dedicated bio-imaging beamline at the European x-ray FEL", *DESY 12-082*, 2012, Available: <http://arxiv.org/abs/1205.6345>.
- [22] G. Geloni et al., "Optimization of a dedicated bio-imaging beamline at the European x-ray FEL", *DESY 12-159*, 2012, Available: <http://arxiv.org/abs/1209.5972>.
- [23] D. Xiang et al., "Purified self-amplified spontaneous emission free-electron lasers with slippage-boosted filtering", *Phys. Rev. ST Accel. Beams*, vol. 16, p. 010703, 2013.
- [24] R. Bonifacio et al., "Large harmonic bunching in a high-gain free-electron laser", *Nucl. Instrum. Methods Phys. Res., Sect. A*, vol. 293, pp. 627-629, 1990.
- [25] Z. Huang and K. Kim, "Three-dimensional analysis of harmonic generation in high-gain free-electron lasers", *Phys. Rev. E*, vol. 62, p. 7295, 2000.
- [26] J. B. Murphy et al., "Collective instability of a free electron laser including space charge and harmonics", *Opt. Commun.*, vol. 53, p. 197, 1985.
- [27] B. W. J. McNeil et al., "Harmonic Lasing in a Free-Electron-Laser Amplifier", *Phys. Rev. Lett.*, vol. 96, p. 084801, 2006.
- [28] E. A. Schneidmiller and M. V. Yurkov, "Harmonic lasing in x-ray free electron lasers", *Phys. Rev. ST Accel. Beams*, vol. 15, p. 080702, 2012.
- [29] S. Serkez et al., "Purified SASE undulator configuration to enhance the performance of the soft x-ray beamline at the European XFEL", *DESY 13-135*, 2013, Available: <http://arxiv.org/abs/1308.0172>.
- [30] S. Reiche et al., "GENESIS 1.3: a fully 3D time-dependent FEL simulation code", *Nucl. Instr. and Meth., ser. A*, vol. 429, pp. 243-248, 1999.
- [31] I. Zagorodnov. (2011). "Beam Dynamics simulations for XFEL" [Online], Available: <http://www.desy.de/fel-beam/s2e>. and "Compression scenarios for the European XFEL" [Online], Available: [http://www.desy.de/fel-beam/data/talks/files/Zagorodnov\\_ACC2012\\_ready\\_new.pptx](http://www.desy.de/fel-beam/data/talks/files/Zagorodnov_ACC2012_ready_new.pptx), 2012.
- [32] Th. Tschentscher, "Layout of the x-Ray Systems at the European XFEL", *Technical Report 10.3204/XFEL.EU/TR-2011-001*, Hamburg, 2011, doi:10.3204/XFEL.EU/TR-2011-001